Influence of Substrates and MgADP on the Time-Resolved Intrinsic Fluorescence of Phosphofructokinase from *Escherichia coli*. Correlation of Tryptophan Dynamics to Coupling Entropy†

Jason L. Johnson and Gregory D. Reinhart*

Department of Chemistry and Biochemistry, University of Oklahoma, Norman, Oklahoma 73019

Received October 6, 1993; Revised Manuscript Received December 22, 1993®

ABSTRACT: The influence that MgADP and the substrate ligands MgATP and fructose 6-phosphate (Fru-6-P) have on the structure of *E. coli* phosphofructokinase (PFK) in the vicinity of the single tryptophan that exists in each subunit has been examined by employing both steady-state and time-resolved measurements of the tryptophan fluorescence. The accessibility of the tryptophan to iodide quenching is over 1 order of magnitude less than experienced by *N*-acetyltryptophanamide in solution but varies nonetheless with the state of ligation. Most, but not all, of these changes correlate with changes in the degree of local motion available to the tryptophan side chain as determined by steady-state and time-resolved polarization measurements. When the data obtained from differential polarization experiments are fit to a model in which the motion of the tryptophan side chain is able to move with high frequency within a cone of limited amplitude as part of an otherwise slowly tumbling spherical protein, it was found that ligands primarily affect the amplitude of the available local motion. By interpreting these effects with reference to the disproportionation equilibria which define the negative coupling free energy between MgADP and Fru-6-P and the positive coupling free energy between MgADP and MgATP, it is apparent that changes in the local motion amplitudes correlate with the sign of the component coupling entropy previously determined from van't Hoff analyses (Johnson & Reinhart, 1994). The data give support, therefore, to the hypothesis that allosteric ligands achieve their effects in part from a perturbation of the dynamical properties of an enzyme that influences the entropy contribution to the coupling free energy.

As discussed in the previous paper (Johnson & Reinhart, 1994), MgADP bound to the allosteric site has very different effects on the two substrates of phosphofructokinase (PFK) from *E. coli*; it facilitates the subsequent binding of Fru-6-P whereas it antagonizes the binding of MgATP. The nature and magnitude of these allosteric effects are quantified by the coupling constants Q_{ax1} and Q_{bx1}, respectively, which are defined by

$$Q_{ax1} = \frac{K^{\circ}_{ia}}{K_{ia/x1}} = \frac{K^{\circ}_{ix1}}{K_{ix1/a}} \quad (1)$$

$$Q_{bx1} = \frac{K^{\circ}_{ib}}{K_{ib/x1}} = \frac{K^{\circ}_{ix1}}{K_{ix1/b}} \quad (2)$$

where K°_{ia}, K°_{ib}, and K°_{ix1} represent the thermodynamic dissociation constants of Fru-6-P (A), MgATP (B), and MgADP (X), respectively, from the enzyme in the absence of other ligands. A "1" is appended to the subscript to signify MgADP bound to the allosteric site rather than to the nucleotide portion of the active site, to which it also binds (Johnson & Reinhart, 1994). $K_{ia/x1}$ and $K_{ib/x1}$ represent the dissociation constants pertaining to Fru-6-P and MgATP, respectively, when MgADP remains bound to the enzyme at the allosteric site, while $K_{ix1/a}$ and $K_{ix1/b}$ refer to the dissociation of MgADP while Fru-6-P and MgATP, respectively, remain bound. Q_{ax1} and Q_{bx1} are equal to 5.5 and 0.072, respectively (Johnson & Reinhart, 1994).

From the definitions given in eqs 1 and 2 it can be easily shown that Q_{ax1} and Q_{bx1} are the equilibrium constants of the following disproportionation reactions

$$\text{MgADP–PFK} + \text{PFK–Fru-6-P} \overset{Q_{ax1}}{\rightleftharpoons} \text{MgADP–PFK–Fru-6-P} + \text{PFK} \quad (3)$$

$$\text{MgADP–PFK} + \text{PFK–MgATP} \overset{Q_{bx1}}{\rightleftharpoons} \text{MgADP–PFK–MgATP} + \text{PFK} \quad (4)$$

where MgADP–PFK represents PFK with MgADP bound at the allosteric site, PFK–Fru-6-P represents PFK with Fru-6-P bound to the active site, PFK–MgATP represents PFK with MgATP bound to the active site, and MgADP–PFK–Fru-6-P and MgADP–PFK–MgATP represent the corresponding ternary complexes with MgADP bound to the allosteric site and the indicated substrate bound to the active site.

The standard free energies of these equilibria, termed coupling free energies (Weber, 1972, 1975), are related to both the respective equilibrium constants and their component ΔH and ΔS by the following:

$$\Delta G_{ax1} = -RT \ln(Q_{ax1}) = \Delta H_{ax1} - T\Delta S_{ax1} \quad (5)$$

$$\Delta G_{bx1} = -RT \ln(Q_{bx1}) = \Delta H_{bx1} - T\Delta S_{bx1} \quad (6)$$

† Supported by Grants GM 33216 from the National Institutes of Health and HR0-025 from the Oklahoma Center for the Advancement of Science and Technology. This work was done during the tenure of an Established Investigatorship of the American Heart Association (to G.D.R.).

* Author to whom correspondence should be addressed.

® Abstract published in *Advance ACS Abstracts,* February 1, 1994.

[1] Abbreviations: NATA, *N*-acetyltryptophanamide; PFK, phosphofructokinase; Fru-6-P, fructose 6-phosphate; BCA, bicinchoninic acid; EPPS, *N*-(2-hydroxyethyl)piperazine-*N'*-(3-propanesulfonic acid).

0006-2960/94/0433-2644$04.50/0

The coupling free energy pertaining to the facilitating MgADP–Fru-6-P interaction, ΔG_{ax1}, is equal to −1.0 kcal/mol at 25 °C according to eq 5. van't Hoff analysis of the variation in Q_{ax1} with temperature indicates that ΔH_{ax1} and $T\Delta S_{ax1}$ equal −3.1 and −2.1 kcal/mol at 25 °C, respectively (Johnson & Reinhart, 1994). ΔG_{bx1} pertains to the antagonistic MgADP–MgATP interaction and is equal to +1.5 kcal/mol at 25 °C. Similar van't Hoff analysis yields values of +1.7 and +0.2 kcal/mol at 25 °C for ΔH_{bx1} and $T\Delta S_{bx1}$, respectively (Johnson & Reinhart, 1994). It follows, therefore, that to understand the origins of the actions of MgADP one must attempt to understand the physical and chemical differences between the species appearing in the equilibria depicted in eqs 3 and 4 that give rise to the constituent ΔH and ΔS.

A potentially useful probe to exploit in this effort is the single tryptophan moiety that is present in each of the identical subunits of the PFK tetramer approximately equidistant (~20 Å) between active and effector sites (Shirakihara & Evans, 1988). The fluorescence properties of this tryptophan are sensitive to the state of ligation of the enzyme (Johnson & Reinhart, 1994). This paper reports the further characterization of the fluorescence properties in an effort to characterize the nature of the perturbations in the vicinity of the tryptophan that are engendered by ligand binding. The results suggest that the binding of ligands changes the dynamic as well as conformational properties of the enzyme in ways that appear to correlate with the sign of the coupling entropy associated with the effects of MgADP on Fru-6-P and MgATP binding, indicating that the origin of the coupling entropy may derive from internal motions of the protein and protein–ligand species populations.

MATERIALS AND METHODS

Materials. Phosphofructokinase was purified from *E. coli* K12, carrying the wild-type pfkA gene, obtained as a frozen paste from Grain Products Corp. All chemical reagents used in buffers, PFK purification, and fluorescence assays were of analytical grade, purchased from either Sigma, Fisher, or Aldrich. The Matrex Gel Blue A-agarose resin for affinity chromatography was purchased fron Amicon Corp. The potassium salts of MgADP and Fru-6-P and the sodium salt of ATP were obtained from Sigma. Deionized distilled water was used throughout.

Protein Determination. Protein determinations were accomplished using the BCA protein assay reagent (Smith et al., 1985). Absorbance readings [$\epsilon_{278} = 0.6\ cm^2\ mg^{-1}$ (Kotlarz & Buc, 1977)] agreed with BCA-established protein concentrations.

Generation of Enzyme Ligand Forms. PFK was purified via a modification of the method of Kotlarz and Buc (1982) as described previously (Johnson & Reinhart, 1992). The enzyme forms MgADP–PFK, PFK–Fru-6-P, PFK–MgATP, MgADP–PFK–Fru-6-P, and MgADP–PFK–MgATP were generated via the addition of 2 mM MgADP and/or 1 mM Fru-6-P and/or 0.5 mM MgATP as appropriate. Based upon the ligand dissociation constants determined previously (Johnson & Reinhart, 1994) less than 1% of the PFK would exist in other forms under these conditions with the exception of the combined addition of 0.5 mM MgATP plus 2 mM MgADP, in which case the MgADP–PFK–MgATP form represents 91% and PFK–MgATP represents 9% of the total PFK. The enzyme forms designated MgADP–PFK and MgADP–PFK–Fru-6-P generated in this manner will also have MgADP bound to the active site. However, because MgADP at the active site has been shown not to influence the intensity or polarization of the fluorescence of the intrinsic tryptophan in *E. coli* PFK (Johnson & Reinhart, 1994), its presence in these species has been ignored.

Steady-State Fluorescence Measurements. Steady-state intensity and anisotropy of the intrinsic PFK fluorescence was measured on an ISS Model K2 multifrequency phase fluorometer equipped with digital acquisition electronics and fast Fourier transform data processing capability. A xenon arc lamp provided the excitation source for intensity measurements, while the 300-nm line of a Spectra-Physics Model 2045 argon ion laser was used in polarization measurements. The excitation beam from the laser was passed through a 2-mm-thick Schott WG-290 filter to remove the 275-nm line also produced by this laser in the "deep-UV" mode. In both cases, emission was collected through a 2-mm-thick Schott WG-345 cut-on filter and a Corning 7-54 band-pass filter. All fluorescence studies were performed in 50 mM EPPS–KOH (pH = 8.0), 10 mM $MgCl_2$, 10 mM NH_4Cl, and 0.2 mM EDTA, with a blank correction of the buffer made in both steady-state intensity and polarization experiments. PFK subunit concentration was equal to 0.36 μM for all steady-state measurements.

Frequency–Domain Fluorescence Measurements. Frequency–domain fluorometry was performed on the ISS K2, using the 300-nm line of the Spectra-Physics argon ion laser, as described above. Emission and excitation filters and buffer conditions were identical to those described for the steady-state fluorescence measurements, while the PFK subunit concentration was 5.7–8.6 μM. All measurements were performed in a 1-cm × 1-cm cuvette with continuous stirring to minimize sample photobleaching. Fluorescence lifetime measurements were performed with excitation (Glan Taylor) and emission (Glan Thompson) polarizers oriented at angles of 0° and 55° to the vertical laboratory axis, respectively, to avoid polarization artifacts (Spencer & Weber, 1970). Correction of frequency–domain measurements for contributions of spurious fluorescence and scatter originating from buffer blanks (Reinhart et al., 1991) was found to have no effect on the results and therefore was not routinely performed. Data analysis was performed with Globals Unlimited, obtained from the Laboratory for Fluorescence Dynamics at the University of Illinois at Urbana-Champaign.

Iodide Quenching. Frequency–domain phase and modulation measurements were performed on each of the six enzyme forms individually in the presence of 0, 0.05, 0.1, and 0.15 M KI. In control experiments increasing in ionic strength to 0.25 M with KCl failed to alter the fluorescence lifetime of the various ligated forms of PFK (data not shown). All data sets were globally linked in terms of the percent of each species in solution and fit using the Globals Unlimited program to the following equation

$$\tau^\circ/\tau = 1 + \tau^\circ k_{sv}[Q] \qquad (7)$$

where τ° represents the lifetime in the absence of quencher, τ represents the apparent lifetime at a given concentration of quencher, Q, and k_{sv} is the Stern–Volmer bimolecular collisional rate constant pertaining to the collision of Q with the excited state of the fluorescent species.

RESULTS

To understand the actions of MgADP with respect to its influence on the binding of each substrate, Fru-6-P and MgATP, we must understand the equilibria depicted in eqs

3 and 4. That is, we must endeavor to understand the basis for the differences in chemical potential of the participating protein species that gives rise to the thermodynamic features that characterize these equilibria. In particular, we wish to consider the possibility that the change in entropy associated with these equilibria may be influenced by changes in structural substate degeneracy (Ansari et al., 1985) that may be reflected in the dynamical properties of the enzyme forms depicted (Reinhart et al., 1989). The following data characterize the fluorescence properties of *E. coli* PFK's single tryptophan moiety, which is located in a position removed from both substrate and allosteric ligand binding sites and slightly exposed to the surface of the enzyme tetramer (Shirakihara & Evans, 1988). The nature of these data provides a characterization of the structural differences between the depicted enzyme forms in the vicinity of the tryptophan sidechain.

Tryptophan Lifetime. The frequency dependence of the phase and modulation of the tryptophan fluorescence of the six unique enzyme forms depicted in eqs 3 and 4 are presented in Figure 1A and 1B, and the corresponding lifetimes implied by these data are presented in Table 1. In all cases, the phase and modulation data were fit best to a model providing for two discrete exponential decays, with the majority of fluorescence intensity (>95%) resulting from the longer component, ranging from 5.2 to 6.3 ns. The lifetime of the short component proved to be relatively invariant in all samples whereas the long component exhibited significant variation with the state of ligation of the enzyme. These observations, together with the iodide quenching results described below and its persistence even after spurious contributions from a buffer blank have been subtracted, suggest that the ubiquitous short component is likely produced by a contaminant of the enzyme stock solution whereas the long component is produced by the tryptophan in PFK. Consequently, the data were analyzed with the minor component's lifetime linked across all data sets, and it was determined to be 1.67 ± 0.26 ns. The long component lifetime and its fractional contribution to the total fluorescence are presented in Table 1 for each enzyme form. As noted previously (Johnson & Reinhart, 1992, 1994), the binding, of either MgADP or Fru-6-P cause the lifetime to decrease significantly. MgATP causes a small increase in the tryptophan lifetime. When both MgADP and Fru-6-P are bound the lifetime is only slightly different from the lifetime obtained with either ligand alone, whereas the lifetime of MgADP–PFK–MgATP is intermediate between the values obtained for the singly-ligated forms. These lifetime variations mimic the commensurate changes in intrinsic fluorescence intensity that follow the binding of these ligands (Johnson & Reinhart, 1994). However, the ligand-induced changes in fluorescence decay times cannot explain the corresponding changes in steady-state polarization that accompany ligand binding (Johnson & Reinhart, 1994), an explanation of which must therefore also include changes in the rotational characteristics of the tryptophan.

Iodide Quenching. Iodide quenching studies of the lifetime of the tryptophan fluorescence decay reveal further distinguishing characteristics between each ligated form of *E. coli* PFK depicted in eqs 3 and 4. The response of the long lifetime fluorescence component to KI is displayed in Figure 2A and 2B. Analysis of these data enables one to determine the bimolecular rate constant, k_{sv}, describing the collision between the quenching molecule, I^-, and the excited state of the tryptophan according to eq 7. The fluorescence decay at all KI concentrations fits best to two exponentials, with greater than 90% of the emission deriving from the longer lifetime

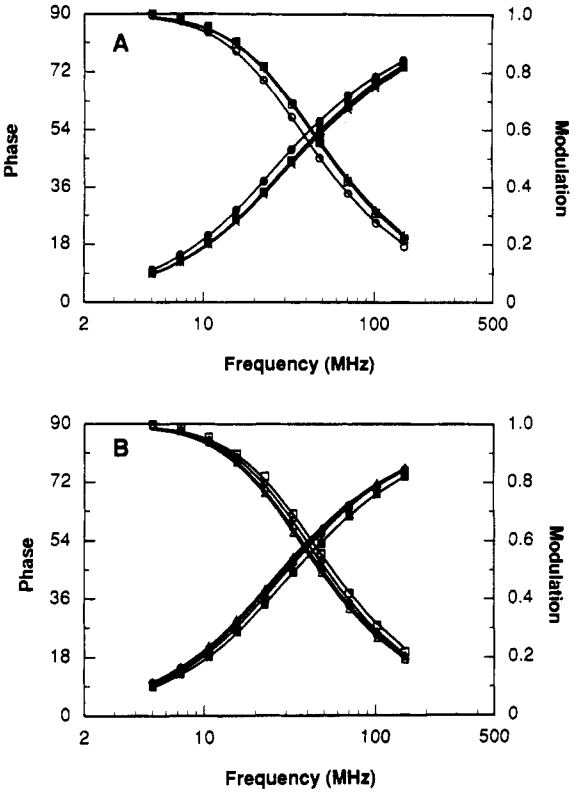

FIGURE 1: Variation of phase and modulation with frequency for each of the enzyme forms appearing in the disproportionation equilibria describing MgADP activation of Fru-6-P binding (A) and inhibition of MgATP binding (B). The phase and modulation for Fru-6-P–PFK–MgADP is represented by (×) and (+), for PFK–Fru-6-P by (▼) and (▽), for PFK by (●) and (○), for PFK–MgADP by (■) and (□), for PFK–MgATP by (▲) and (△), and for MgATP–PFK–MgADP by (◆) and (◇), respectively. The lines drawn represent the best fit of the data to a model of two discrete exponential lifetimes, with the small percentage component linked across data sets. Results of these analyses are listed in Table 1.

component as described above. The shorter component was not only independent of ligation but also quenched with a k_{sv} comparable to that of NATA (3.3 ± 1.0 M^{-1} ns^{-1} vs 4.7 ± 0.1 M^{-1} ns^{-1}, respectively), suggesting that it originates from a contaminant of the *E. coli* PFK preparation that is not associated with *E. coli* PFK itself.

The tryptophan in *E. coli* PFK is largely, but not completely, inaccessible to I^- quenching as indicated by the small value of k_{sv} associated with the major component of the fluorescence decay relative to that for NATA, consistent with its location as determined by X-ray crystallography (Shirakihara & Evans, 1988). Nonetheless, though small, the k_{sv} is dependent upon the state of ligation of the enzyme. The binding of Fru-6-P and MgADP, both individually and in combination, cause k_{sv} to increase, indicating that the tryptophan becomes more accessible to I^-, with Fru-6-P along having the greatest effect. The PFK–MgATP and MgATP–PFK–MgADP, on the other hand, display decreases in k_{sv} relative to free enzyme, with MgATP–PFK–MgADP exhibiting the smallest k_{sv}, suggesting that tryptophan in this enzyme form is the least accessible to I^- of the forms examined. Values of k_{sv} for each complex are summarized in Table 1.

Steady-State Fluorescence Polarization. As mentioned previously (Johnson & Reinhart, 1994) the value of the steady-state polarization of *E. coli* PFK's intrinsic fluorescence is also influenced by its state of ligation. That this variation is not due to changes in fluorescence lifetime resulting from ligand binding is demonstrated in Figure 3 in which the

Table 1: Biophysical Parameters Describing Enzyme Complexes Relevant to the Net Allosteric Responses of *E. coli* PFK to the Effector MgADP[a]

complex	τ^b (ns)	f_1	P_o	k_{sv} (M·ns)$^{-1}$	$r_0 - r_\infty{}^c$	Φ (deg)
PFK	5.94 ± 0.08	0.930 ± 0.007	0.363 ± 0.002	0.13 ± 0.04	0.030 ± 0.010	8.2 ± 1.5
PFK–Fru-6-P	5.23 ± 0.07	0.917 ± 0.008	0.330 ± 0.001	0.34 ± 0.05	0.123 ± 0.010	16.9 ± 0.8
PFK–MgATP	6.15 ± 0.09	0.937 ± 0.006	0.377 ± 0.002	0.11 ± 0.02	0.015 ± 0.009	5.7 ± 1.8
MgADP–PFK	5.30 ± 0.08	0.903 ± 0.008	0.364 ± 0.002	0.21 ± 0.04	0.030 ± 0.010	8.2 ± 1.5
MgADP–PFK–Fru-6-P	5.21 ± 0.08	0.900 ± 0.009	0.358 ± 0.001	0.26 ± 0.05	0.060 ± 0.009	11.6 ± 0.9
MgADP–PFK–MgATP	5.55 ± 0.07	0.943 ± 0.008	0.364 ± 0.003	0.08 ± 0.02	0.060 ± 0.009	11.6 ± 0.9

[a] Symbols used in this table correspond to the following parameters: τ, fluorescence lifetime of major component; f_1, fractional intensity of the major component; P_o, apparent limiting polarization as measured by Perrin plots; k_{sv}, bimolecular rate constant pertaining to quenching by I^-; $r_0 - r_\infty$, preexponential amplitude for fast rotation; and Φ, cone angle of local rotation. [b] Data were analyzed with a second lifetime component, τ_2, linked across all data sets. τ_2 = 1.67 ± 0.26 ns; global χ^2 = 2.31. [c] Data were fit to eq 8 described in the text. The parameters ϕ_1, ϕ_2, and r_0 were linked across all data sets and found to be equal to 0.80 ± 0.15 ns, 76 ± 5 ns, and 0.26 ± 0.02, respectively. Global χ^2 = 0.75.

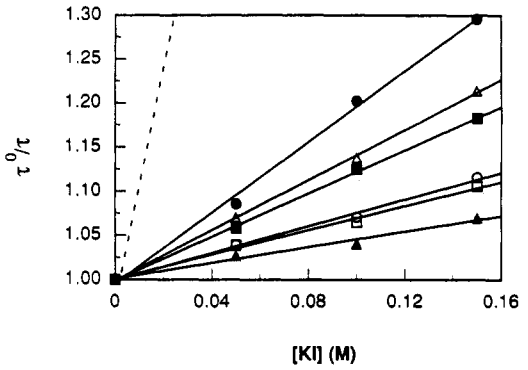

FIGURE 2: Variation in fluorescence lifetime, determined as in Figure 1, with iodide ion concentration for PFK bound to no ligands (○), to Fru-6-P (●), to MgATP (□), to MgADP (■), to Fru-6-P and MgADP (△), and to MgATP and MgADP (▲). The dashed line represents the response of the lifetime of NATA free in solution to I^- quenching. All data sets were globally linked in terms of the percent of each species in solution and fit using Globals Unlimited to eq 7 described in the text. The bimolecular rate constant (k_{sv}) associated with collisional quenching is obtained from the slopes of the lines divided by τ^0, the lifetime in the absence of I^-, given in Table 1. In general, it was found that those species exhibiting shorter lifetimes were correspondingly more exposed to iodide quenching, with the notable exception of MgADP–PFK–MgATP.

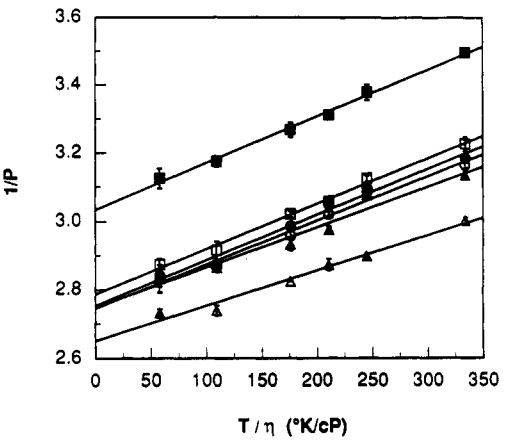

FIGURE 3: Effects of isothermally varying solution viscosity (η) with sucrose on the steady-state polarization of PFK bound to no ligands (●), to Fru-6-P (■), to MgATP (△), to MgADP (○), to Fru-6-P and MgADP (□), and to MgATP and MgADP (▲) at 25 °C. Plots of $1/P$ vs T/η extrapolated to infinite viscosity provide values for the apparent limiting polarization (P_o), which are summarized in Table 1.

variation of steady-state polarization as a function of viscosity, η, is presented in the form of a "Perrin plot" (Weber, 1952). These data indicate that the polarization differences are virtually entirely manifest in changes in the apparent Y-axis intercept, i.e., the apparent P_o value obtained after extrapolating to infinite solution viscosity. The slope of a Perrin plot is related to the rotational relaxation time of the protein as a whole, whereas differences in the Y-axis intercept reflect changes in depolarization mechanisms that are independent of solvent viscosity, such as energy transfer or local intramolecular rotations of the tryptophan side chain (Weber, 1952). The apparent values of P_o obtained from the Y-axis intercepts of the Perrin plots for the six enzyme forms appearing in eqs 1 and 2 are presented in Table 1.

Differential Polarization. Differential polarized phase/modulation fluorometry, unlike steady-state polarization measurements, can discriminate between and quantify the discrete modes of rotation, e.g., global vs local rotation, available to a fluorescent moiety. The frequency spectrum of the differential phase and modulation of the intrinsic tryptophan fluorescence of the four enzyme forms that establish the coupling between MgADP and Fru-6-P (i.e., eq 3) are shown in Figure 4A. Similar data pertaining to the coupling between MgADP and MgATP are shown in Figure 4B. Although the state of ligation has only a small effect on the data in Figure 4B, the differences between the curves in Figure 4A are quite significant, since the data were collected to an average precision of ±0.06° phase and ±0.001 modulation. To further verify that the changes in Figure 4A are significant, titrations were performed at 75 MHz as shown in Figure 5. By taking advantage of the ISS digital data acquisition electronics and collecting data for roughly 20–30 min per data point, differential phase was determined to a precision of ±0.02°. Clearly, as Fru-6-P is added to free enzyme, the differential phase increaes in a continuous manner, whereas when MgADP is added to free enzyme the differential phase decreases slightly. Adding the second ligand brings about a common value for the differential phase corresponding to the ternary complex.

The curves drawn in Figure 4 represent the best fit of each data set to a hindered local motion plus global rotation model (Munro et al., 1979; Lipari & Szabo, 1980)

$$r(t) = (r_o - r_\infty)e^{-t/\phi_1} + r_\infty e^{-t/\phi_2} \quad (8)$$

where r_o is the anisotropy at $t = 0$, ϕ_1 and ϕ_2 are rotational correlation times associated with two modes of rotation such that $\phi_1 \ll \phi_2$, and r_∞ equals the anisotropy that persists at times long relative to the short rotational correlation time, ϕ_1. When double exponentials are evident, the depolarization amplitude of the fast rotation must be limited (i.e., $r_\infty > 0$). When such a hindered fast rotation is modeled as rotation within a cone, the cone angle, Φ, describing the amplitude of restricted motion is given by (Munro et al., 1979; Lipari & Szabo, 1980; Gratton et al., 1986):

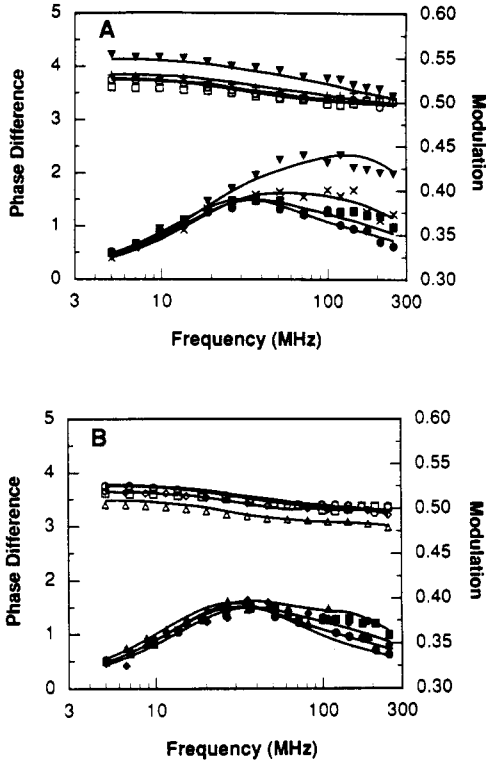

FIGURE 4: Frequency spectra of the differential phase and modulation of the intrinsic tryptophan fluorescence of those species pertinent to net activation of Fru-6-P binding by MgADP (A) and net inhibition of MgATP binding by MgADP (B). The differential phase and modulation for MgADP–PFK–Fru-6-P is represented by (×) and (+), for PFK–Fru-6-P by (▼) and (▽), for PFK by (●) and (○), for MgADP–PFK by (■) and (□), for PFK–MgATP by (▲) and (△), and for MgADP–PFK–MgATP by (◆) and (◇), respectively. The curves represent the best fit of the data to a hindered local motion (ϕ_1) plus global protein rotation (ϕ_2). Independent analysis of each data set indicates that differences in each spectrum arise principally from changes in the amplitude of local rotation of the tryptophan moiety. Therefore, ϕ_1, ϕ_2, and r_0 were linked during global analysis of the four data sets, while the lifetimes were fixed to the major component obtained from the data in Figure 1. Results of these analyses are given in Table 1.

$$\Phi = \cos^{-1}\left(\frac{1}{2}\left\{\left[1 + 8\left(\frac{r_\infty}{r_0}\right)^{1/2}\right]^{1/2} - 1\right\}\right) \qquad (9)$$

When analyzed independently, little difference was seen between the rotational relaxation times associated with either global (ϕ_2) or local (ϕ_1) rotational correlation times in any of the six enzyme complexes. Instead, the presence of ligands predominantly affects the amplitudes of rotation available to the tryptophan in *E. coli* PFK. For this reason, a global analysis was performed across all six data sets in which ϕ_1 and ϕ_2, as well as r_0 which is independent of rotational mechanism,

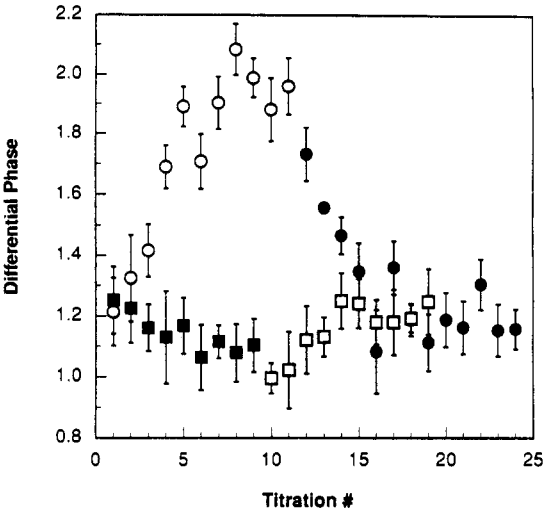

FIGURE 5: Variation of differential phase at 75 MHz with Fru-6-P and MgADP concentration. Unligated PFK was titrated with Fru-6-P (○) followed by the addition of successive amounts of MgADP (●). Alternatively, unligated PFK was titrated with MgADP (■) followed by Fru-6-P (□). Titration no. represents a constant multiple increase in concentration of the corresponding ligand.

were linked. Lifetimes for each enzyme form were fixed during analysis to the values of the major component for each species determined from the data in Figures 1. Analysis in this manner[2] achieved an overall χ^2 of 0.75. The following values were obtained for the linked parameters: $r_0 = 0.26 \pm 0.02$, $\phi_1 = 0.80 \pm 0.15$ ns, and $\phi_2 = 76 \pm 5$ ns. The amplitude of the local rotational component, $r_0 - r_\infty$, was found to be ligand dependent, and the values obtained for each of the species appearing in eqs 3 and 4 are presented in Table 1. In addition, the amplitude is also given in Table 1 as the cone angle associated with the local motion that was calculated from the values of r_0 and r_∞ according to eq 9.

DISCUSSION

For the four species appearing in the disproportionation reaction (eq 3) describing net allosteric activation of Fru-6-P affinity by MgADP, the concerted two-state model for interpreting allosteric behavior would predict that all of these forms correspond to the R state (Monod et al., 1965; Blangy et al., 1968), with the possible exception of the unligated enzyme which has been proposed to exist as a mixed population of R and T forms (Deville-Bonne & Garel, 1992). However, although Fru-6-P and MgADP decrease the fluorescence intensity of *E. coli* PFK's single tryptophan per subunit similarly, purportedly ascribed to an increase in the population of the R conformation (Berger & Evans, 1991; Deville-Bonne & Garel, 1992), rigorous analysis of the fluorescence characteristics of the protein bound to substrate and allosteric ligand, both separately and in combination, reveals several distinctions between these enzyme forms. Similar types of differences are seen between the species participating in eq 4. In particular, the accessibility of solvent as measured by I^- quenching and the rotational characteristics of the intrinsic tryptophan are unique to each state of ligation.

Stern–Volmer analysis of the accessibility of the tryptophan's fluorescence decay to iodide quenching reveals that the bimolecular quenching rate constant for all of the enzyme forms appearing in both eqs 3 and 4 is small relative to that for NATA free in solution, as expected given the limited exposure of the tryptophan to the surface of the *E. coli* PFK (Shirakihara & Evans, 1988). Significant changes in the limited accessibility of the tryptophan to I^- as a function of

[2] A variety of models were examined in an attempt to incorporate the minor lifetime component in the analysis of the decay of anisotropy. These models included schemes in which this component was either associated with its own decay or the decay associated with the major lifetime component. Since the differential phase and modulation values change so little with frequency, and the contribution of the short component is such a minor contributor to the total fluorescence throughout the frequency range examined, too little information is available in these measurements to establish any sensible basis for assessing the contribution that the minor lifetime component makes to the anisotropy characteristics or for distinguishing between these alternative models. In addition, although some of these attempts resulted in a small reduction in the overall χ^2, they had no significant impact on the preexponential terms associated with the major component obtained when the short component was simply ignored in the analysis.

the enzyme's state of ligation can be discerned, however. The tryptophan of PFK bound to Fru-6-P is approximately three times more accessible than that of unligated enzyme. The tryptophan of the ternary complex of MgADP–PFK–Fru-6-P is quenched 2-fold more readily than is free PFK, while accessibility to iodide ions for the MgADP–PFK complex lies between free enzyme and the ternary complex. The picture is somewhat different with respect to the enzyme forms pertinent to eq 4 describing the MgADP–MgATP coupling. The tryptophans in both PFK–MgATP and MgADP–PFK–MgATP exhibit diminished accessibility to I^- compared to free enzyme, although the difference is of questionable significance.

Steady-state and time-resolved analysis of the fluorescence polarization of *E. coli* PFK's single tryptophan reveal similarly distinct features between the enzyme ligated to Fru-6-P, MgATP, and MgADP separately and in combination. The apparent limiting polarization values (P_o) for each of the enzyme forms determined from the isothermal variation of solution viscosity with sucrose indicate that differences in the steady-state polarization values derive at least in part from differences in the local rotation of the tryptophan (Weber, 1952). Energy transfer between the four tryptophans in the tetramer is not likely to occur because of the red-edge excitation wavelength (300 nm) used. Differential polarized phase/modulation fluorometry further indicates that variations in the local rotation of the tryptophan indeed represent the primary differences between tryptophan motions in each enzyme complex, and these differences arise principally from changes in the amplitude of local rotation available to the tryptophan. Limited-amplitude fast motion of this type has often been described with a model in which the tryptophan moves rapidly within a cone of available space within the protein matrix (Munro et al., 1979; Lipari & Szabo, 1980; Gratton et al., 1986). When such a model is applied to our data, the most notable result is the much larger cone angle measured for the PFK–Fru-6-P enzyme form relative to those of the other species (Table 1). This larger amplitude correlates qualitatively with the greater accessibility of the tryptophan to I^- quenching also exhibited by this enzyme form. Indeed, the relative differences in the local amplitude of tryptophan motion of each of the enzyme forms appearing in the MgADP–Fru-6-P coupling equilibrium depicted in eq 3 correlates qualitatively with the values of k_{sv} determined by I^- quenching. However, a similar correlation is not evident with the species participating in the MgATP–MgADP coupling equilibrium (eq 4) underscoring the fact that local motion changes do not require increased exposure of the tryptophan to the surface of the protein.

It has been shown that the coupling entropy term ($T\Delta S$) is instrumental in establishing the degree to which MgADP allosterically enhances Fru-6-P affinity and antagonizes MgATP binding to *E. coli* PFK (Johnson & Reinhart, 1994). For example, the nature of the changes produced in either coupling when the second substrate binds derives exclusively from the changes in the coupling entropy (Johnson & Reinhart, 1994). Such basic involvement of $T\Delta S$ in the allosteric features of *E. coli* PFK brings to focus the importance of assessing the possible molecular origins of coupling entropy. In this regard, solvent effects may not play a substantial role, since the disproportionation reaction involves species containing the same number of empty and filled binding sites and does not involve free ligand (Reinhart et al., 1989). Additionally, heat capacity changes, which are generally associated with changes in the degree of solvation (Sturtevant, 1977), were not observed to a significant extent in the pertinent van't Hoff plots (Johnson & Reinhart, 1994). The linearity of these plots suggests that the entropy term may derive from a characteristic of the protein matrix that is responsive to ligation by small molecular weight ligands. Indeed, it has been previously speculated (Cooper & Dryden, 1984; Reinhart et al., 1989) that differences in entropy between those species in eqs 3 and 4 derive from differences in the flexibility of the protein and its related ability to populate various configurational substates (Ansari et al., 1985).

Frequency–domain anisotropy measurements have provided a means to monitor and compare the degree of flexibility associated with the tryptophan side chain in each of those species appearing in the disproportionation equilibrium for MgADP-mediated activation of Fru-6-P binding and inhibition of MgATP binding. Indeed, for the MgADP–Fru-6-P coupling, greater flexibility is demonstrated for those species on the *left* of the disporportionation reaction, qualitatively agreeing with the negative sign of ΔS_{ax1} measured for this equilibrium (Johnson & Reinhart, 1994). This agreement can be seen by considering the cone angles within the context of eq 3:

$$\begin{array}{lccc} & & & \overset{\Delta S_{ax1} < 0}{\rightleftharpoons} \\ & \text{MgADP–PFK} + \text{PFK–Fru-6-P} & & \\ \text{cone angles:} & (8°) \quad (17°) & & \\ & & \text{MgADP–PFK–Fru-6-P} + \text{PFK} & \\ & & (12°) \quad (8°) & \end{array}$$

The tryptophans in unligated PFK and MgADP–PFK exhibit similar amplitudes of local motion and effectively cancel each other's contribution to the equilibrium, while the PFK–Fru-6-P complex displays greater flexibility of the side chain than does that of MgADP–PFK–Fru-6-P.

Similarly, for the MgATP–MgADP coupling, greater flexibility is demonstrated for those species on the *right* of the disproportionation reaction (eq 4), consistent with the positive sign of ΔS_{bx1} observed for this equilibrium (Johnson & Reinhart, 1994):

$$\begin{array}{lccc} & & & \overset{\Delta S_{bx1} > 0}{\rightleftharpoons} \\ & \text{MgADP–PFK} + \text{PFK–MgATP} & & \\ \text{cone angles:} & (8°) \quad (6°) & & \\ & & \text{MgADP–PFK–MgATP} + \text{PFK} & \\ & & (12°) \quad (8°) & \end{array}$$

In this case, it is the restricted flexibility of the MgATP-bound complex relative to the ternary complex which produces a difference between the two sides of the equilibrium.

Together, these correlations of protein flexibility and the associated sign of the coupling entropy suggest that the coupling entropy, which is important in establishing the magnitude of the allosteric effect in *E. coli* PFK (Johnson & Reinhart, 1994), may indeed derive from the perturbations of enzyme dynamics that result from the binding of allosteric and substrate ligands. For these correlations to be more than just suggestive, however, further evidence for a global effect on the dynamic properties of the enzyme must be obtained.

REFERENCES

Ansari, A., Berendzen, J., Bowne, S. F., Frauenfelder, H., Iben, I. E. T., Sauke, T. B., Shyamsunder, E., & Young, R. D. (1985) *Proc. Natl. Acad. Sci. U.S.A. 82*, 5000–5004.

Berger, S. A., & Evans, P. R. (1991) *Biochemistry 30*, 8477–8480.

Blangy, D., Buc, H., & Monod, J. (1968) *J. Mol. Biol. 31*, 13–35.

Cooper, A., & Dryden, D. T. F. (1984) *Eur. Biophys. J. 11*, 103–109.

Deville-Bonne, D., & Garel, J.-R. (1992) *Biochemistry 31*, 1695–1700.
Gratton, E., Alcala, J. R., & Marriott, G. (1986) *Biochem. Soc. Trans. 14*, 835–838.
Johnson, J. L., & Reinhart, G. D. (1992) *Biochemistry 31*, 11510–11518.
Johnson, J. L., & Reinhart, G. D. (1994) *Biochemistry* (previous paper in this issue).
Kotlarz, D., & Buc, H. (1977) *Biochim. Biophys. Acta 484*, 35–48.
Kotlarz, D., & Buc, H. (1982) *Methods Enzymol. 90*, 60–70.
Lipari, G. & Szabo, A. (1980) *Biophys. J. 30*, 489–506.
Monod, J., Wyman, J., & Changeux, J. P. (1965) *J. Mol. Biol. 3*, 318–356.
Munro, I., Pecht, I., & Stryer, L. (1979) *Proc. Natl. Acad. Sci. U.S.A. 76*, 56–60.
Reinhart, G. D., Hartleip, S. B., & Symcox, M. M. (1989) *Proc. Natl. Acad. Sci. U.S.A. 86*, 4032–4036.
Reinhart, G. D., Marzola, P., Jameson, D. M., & Gratton, E. (1991) *J. Fluoresc. 1*, 153–162.
Shirakihara, Y., & Evans, P. R. (1988) *J. Mol. Biol. 204*, 973–994.
Smith, D. K., Krohn, R. I., Hermanson, G. T., Mallia, A. K., Gartner, F. H., Provenzano, M. D., Fujimoto, E. K., Goeke, N. M., Olson, B. J., & Klenk, B. C. (1985) *Anal. Biochem. 150*, 76–85.
Spencer, R. D., & Weber, G. (1970) *J. Chem. Phys. 52*, 1654–1663.
Sturtevant, J. M. (1977) *Proc. Natl. Acad. Sci. U.S.A. 74*, 2236–2240.
Weber, G. (1952) *Biochem. J. 51*, 145–155.
Weber, G. (1972) *Biochemistry 11*, 864–878.
Weber, G. (1975) *Adv. Protein Chem. 29*, 1–83.